

1

2 **Electronic Supplementary Information:**

3

4 **Self-Propelling Shuttles for Radioactive Caesium Adsorption**

5

6 Richard I. Foster,<sup>‡a</sup> Hyung-Ju Kim,<sup>‡\*b</sup> Sung-Jun Kim,<sup>b</sup> Chan Woo Park,<sup>b</sup> Hee-Man Yang<sup>b</sup> and

7 Jung-Hyun Lee<sup>\*c</sup>

8

9 <sup>a</sup>Nuclear Research Institute for Future Technology and Policy, Seoul National University, 1

10 Gwanak-ro, Gwanak-gu, Seoul 08826, Republic of Korea

11 <sup>b</sup>Decommissioning Technology Research Division, Korea Atomic Energy Research Institute,

12 989-111 Daedeok-daero, Yuseong-gu, Daejeon 34057, Republic of Korea

13 <sup>c</sup>Department of Chemical and Biological Engineering, Korea University, 145 Anam-ro,

14 Seongbuk-gu, Seoul 02841, Republic of Korea

15 **\*Corresponding Author**

16 H.J. Kim, E-mail: hyungjukim@kaeri.re.kr

17 J.H. Lee, E-mail: leejhyyy@korea.ac.kr

18 <sup>‡</sup>Authors have contributed equally to this work.

19 Pages: 22

20 Tables: 3

21 Figures: 12

22 Movie: 1

## 23 I. Materials and Methods

### 24 Materials

25 PVC tube (Saint Gobain Tygon S3™, E-3603 Flexible Tube, Special PVC), 1.59 mm ID  
26 × 3.18 mm OD, forming the shuttle shell was used. Tris(hydroxymethyl)aminomethane, dopamine  
27 hydrochloride, acrylamide, N, N'-methylenebisacrylamide, 2,2-dimethoxy-2-  
28 phenylacetophenone, iron (III) chloride hexahydrate, potassium (II) ferrocyanide trihydrate, and  
29 iron (III) ferrocyanide (PB), were purchased from Sigma-Aldrich. Inductively coupled plasma  
30 (ICP) Cs standard solution (1000 ppm), ethanol (94.5%), and nitric acid (65%) were purchased  
31 from AccuStandard, Samchun, and Merck, respectively. All chemicals were used as received  
32 without further purification. Deionized (DI) water (18.2 MΩ cm at 25 °C), was obtained from a  
33 Millipore Milli-Q Academic water purification system.

34

### 35 Preparation of the PB-containing PVC tube shuttle

36 **Dopamine Coating:** Dopamine (D) was coated on the surface of the plastic PVC tube. The  
37 dopamine coating was utilised because of its high adhesive property,<sup>1</sup> which enabled the strong  
38 binding to both PB and PVC tube surface. To achieve this, solutions of dopamine hydrochloride  
39 ( $2.64 \times 10^{-3}$  M) and tris(hydroxymethyl)-aminomethane ( $2.0 \times 10^{-3}$  M) were prepared in DI water  
40 (300 mL). The plastic tube with a length of 150 mm was then immersed in the prepared dopamine  
41 solution while stirring at room temperature for 24 h, during which time self-polymerisation of the  
42 dopamine coated the tube surface. Subsequently, the dopamine-coated tube, denoted as Tube-D,  
43 was rinsed with DI water. **Prussian Blue Functionalisation:** Tube-D was functionalised with PB  
44 for the purpose of selectively removing Cs. To achieve this, Tube-D was immersed in an aqueous  
45 solution (200 mL) of iron (III) chloride hexahydrate (either 0.09, 0.18, 0.36, or 1 M) and stirred at

46 room temperature for 24 h. An aqueous solution (200 mL) of potassium hexacyanoferrate (II)  
47 trihydrate (either 0.06, 0.11, 0.22, or 0.5 M) was then added to the stirring mixture and stirred for  
48 a further 24 h. Finally, the tube was rinsed with DI water until the water ran clear, followed by  
49 drying in a desiccator at room temperature overnight to obtain the PB-functionalised tube, denoted  
50 as Tube-D-PB. **Self-propelling Shuttle:** Tube-D-PB prepared with diverse precursor  
51 concentrations, as described above, were cut into lengths of 20 mm to form individual shuttles.  
52 The self-propelling function was imparted to the Tube-D-PB by injecting ethanol-infused hydrogel  
53 into the tube as described in elsewhere.<sup>2</sup> Ethanol was chosen as it is benign and easily evaporates  
54 due to being volatile, thus does not require separation from the aqueous system. The ethanol-  
55 infused hydrogel was prepared by dissolving acrylamide (monomer), N,N'-  
56 methylenebisacrylamide (cross-linker), and 2,2-dimethoxy-2-phenylacetophenone (initiator) with  
57 a weight ratio of 1:0.1:0.01 in an equivolume mixture (50 vol% of ethanol) of ethanol and water.  
58 The prepared solution mixture was injected manually using a syringe into the tube and cured using  
59 a UV lamp (B-100A, Analytikjena, 100 W, emitting wavelength of 356 nm) for 15 minutes.  
60 Dormant shuttles were also prepared as a control without injecting ethanol-infused hydrogel for  
61 comparison.

62

### 63 Characterisation

64 Fourier Transform Infrared (FT-IR) spectroscopy analysis was performed using a Thermo  
65 Nicolet iS5 equipped with Attenuated Total Reflectance to determine the success of dopamine  
66 coating and functionalisation of PB. X-ray diffraction (XRD, D2 PHASER, Bruker) patterns were  
67 collected from 10 to 80° of 2θ at a rate of 0.02° per step with a counting time of 0.2 s per step  
68 using Cu-K-alpha source radiation. High-resolution scanning electron microscopy (HR-SEM,

69 SU8230, Hitachi) was used to examine the morphology of the prepared tube surfaces. Energy  
70 dispersive X-ray spectroscopy (EDS, X-max N80, Horiba) mapping was also performed to identify  
71 the element composition of the sample.

72 The movement of the self-propelling shuttle was recorded with a digital camera (EOS  
73 800D, Canon). To analyse the cumulative distance and velocity of the self-propelling shuttle, the  
74 recorded video was separated by screenshot images taken every specific time interval of 2 s, during  
75 30 s of moving. The screenshot images were combined using Photoshop (CS6 Portable, Adobe) to  
76 display tracer movement as an image overlay. The cumulative distance was presented using the  
77 points from the centre of shuttle, and the velocity was calculated from the first differential of the  
78 cumulative distance.

79

#### 80 Caesium removal test with non-radioactive and radioactive substances

81 The Cs removal test was performed by floating the self-propelling shuttles on 75 mL of 1  
82 ppm Cs aqueous solution in a petri dish at room temperature. There was a total of three systems  
83 studied for the adsorption of non-radioactive Cs ions, a) self-propelling, b) non-stirred, and c)  
84 stirred conditions. For both the non-stirred (b) and stirred (c) systems dormant Tube-D-PB shuttles  
85 were used which were surface functionalised with PB but importantly did not contain the ethanol  
86 infused hydrogel so were incapable of self-motion. Thus, making it possible to investigate the  
87 effect of the self-propelling property of the Tube-D-PB shuttles containing the ethanol-infused  
88 hydrogel on Cs ion adsorption. Removal kinetics were determined by repeating the aforementioned  
89 Cs removal test for predetermined time intervals between 5 and 30 minutes using the optimised  
90 self-propelling shuttle to obtain a kinetic isotherm. Further, Cs removal was performed with  
91 dormant shuttles under both stationary and stirred (500 rpm) conditions, to elucidate the effect of

92 the self-propelling. After every single Cs removal test, the self-propelling shuttle was separated,  
93 and the Cs ion concentration in the residual supernatant solution was analysed using ICP-optical  
94 emission spectroscopy (ICP-OES, PQ9000 Elite, Analytikjena). Cs removal efficiency ( $R$ , %) was  
95 described by the following equation (1):

$$96 \quad R (\%) = \frac{C_0 - C_i}{C_0} \times 100 \quad (1)$$

97 where  $C_0$  is initial Cs ion concentration, and  $C_i$  is final Cs ion concentration.

98 To confirm the validity of the ‘inactive’ results, the removal of radioactive Cs (Isotope:  
99  $^{137}\text{Cs}$ ) was verified. An optimised self-propelled shuttle was floated on 75 mL of  $^{137}\text{Cs}$  aqueous  
100 solution ( $37 \text{ Bq mL}^{-1}$ , equivalent to 11.5 ppt Cs). The activity of  $^{137}\text{Cs}$  in the solution before and  
101 after 30 minutes of adsorption was measured using high-resolution gamma spectrometry (Canberra  
102 Ind.) with a high-purity gamma detector equipped with a multi-channel analyser. The  $^{137}\text{Cs}$   
103 removal efficiency ( $R$ , %) was calculated by substituting the Cs concentration as activity of  $^{137}\text{Cs}$   
104 in equation (1).

105

#### 106 Adsorption isotherms and kinetics

107 Isotherm loading experiments were performed to assess the maximum loading capacity of  
108 the Tube-D-PB. The maximum capacity was determined through linear fitting of common  
109 adsorption isotherm models (Table S2), namely, Langmuir in equation (2), Freundlich in equation  
110 (3), Dubinin-Radushkevich in equation (4), and Tempkin in equation (5); where  $C_e = [\text{Cs}^+]_{(\text{aq})}$  at  
111 equilibrium ( $\text{mg L}^{-1}$ ),  $q_e = [\text{Cs}^+]_{(\text{Tube-D-PB})}$  at equilibrium ( $\text{mg g}^{-1}$ ),  $q_m = [\text{Cs}^+]_{(\text{Tube-D-PB})}$  maximum  
112 capacity ( $\text{mg g}^{-1}$ ),  $K_L = \text{Langmuir isotherm constant (L mg}^{-1})$ ,  $K_F = \text{Freundlich isotherm constant}$ ,  
113  $n_F = \text{Freundlich isotherm adsorption intensity}$ ,  $K_{\text{DR}} = \text{Dubinin-Radushkevich isotherm constant}$

114 ( $\text{mol}^2 \text{J}^{-2}$ ),  $R$  = universal gas constant ( $\text{J mol}^{-1} \text{K}^{-1}$ ),  $T$  = temperature (K),  $K_T$  = Tempkin isotherm  
115 constant, and  $A_T$  = Tempkin isotherm equilibrium binding constant ( $\text{L g}^{-1}$ ).<sup>3,4</sup> Linear fits are shown  
116 in Fig. S11 with fitting parameters for all models shown below (Table S3). Suitability of the fits  
117 was determined by calculating adj.  $R^2$  values.

118

119

120

121

122

123

124

125

126

127

128

129

130

131

132

133

134

135

136

137 **II. Supplementary Tables**

138

139 **Table S1.** The element composition from EDS analysis of Tube, Tube-D, and Tube-D-PB.

Element	Tube (wt%)	Tube-D (wt%)	Tube-D-PB (wt%)
C	70.57	69.45	67.87
N	0.00	0.00	1.39
O	16.68	21.21	19.10
Al	0.36	0.00	0.16
Cl	12.38	9.30	8.85
Fe	0.00	0.00	2.63
Total	100	100	100

140

141

142

143

144

145

146

147

148

149

150

151

152

153 **Table S2.** Summary of isotherm models used.

Isotherm	Non-linear	Linear	Plot	Equation	Ref
Langmuir	$q_e = \frac{q_m K_L C_e}{1 + K_L C_e}$	$\frac{C_e}{q_e} = \frac{C_e}{q_m} + \frac{1}{K_L q_m}$	$C_e$ vs. $\frac{C_e}{q_e}$	(2)	5
Freundlich	$q_e = K_F C_e^{1/n}$	$\ln q_e = \ln K_F + \frac{1}{n} \ln C_e$	$\ln(C_e)$ vs. $\ln(q_e)$	(3)	6
Dubinin-Radushkevich	$q_e = q_m e^{-K_{DR} \left( RT \ln \left( 1 + \frac{1}{C_e} \right) \right)^2}$	$\ln q_e = \ln q_m - K_{DR} \epsilon^2$	$\epsilon^2$ vs. $\ln(q_e)$	(4)	7
Tempkin	$q_e = \frac{RT}{K_T} \ln(A_T C_e)$	$q_e = \frac{RT}{K_T} \ln A_T + \frac{RT}{K_T} \ln C_e$	$\ln(C_e)$ vs. $q_e$	(5)	8

154

155

156

157

158

159

160

161

162

163

164

165

166

167

168

169

170

171

172

173 **Table S3.** Summary of isotherm model fitting parameters for Cs<sup>+</sup> uptake by Tube-D-PB.

Parameters	Adsorption Isotherm			
	Langmuir	Freundlich	Dubinin-Radushkevich	Tempkin
R <sup>2</sup>	0.9958	0.9195	0.6255	0.9059
Adj. R <sup>2</sup>	0.9948	0.8994	0.5319	0.8824
q <sub>m</sub> (mg g <sup>-1</sup> )	106.38	-	95.54	-
K <sub>L</sub> (L mg <sup>-1</sup> )	0.04	-	-	-
K <sub>F</sub>	-	49.68	-	-
N	-	8.75	-	-
K <sub>DR</sub>	-	-	0.00	-
E (kJ mol <sup>-1</sup> )	-	-	73.68	-
K <sub>T</sub>	-	-	-	240.80
A <sub>T</sub>	-	-	-	36.05

174

175

176

177

178

179

180

181

182

183

184

185

186

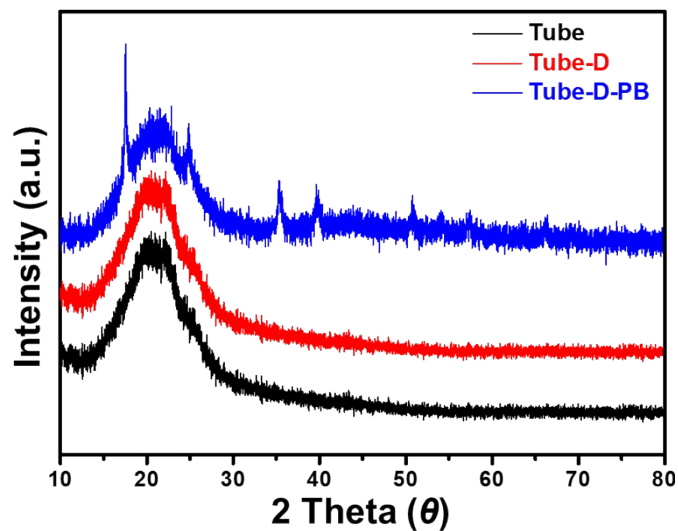
187

188

189

190 **III. Supplementary Figures and Movie**

191



192

193 **Fig. S1.** XRD patterns of the Tube, Tube-D, and Tube-D-PB.

194

195

196

197

198

199

200

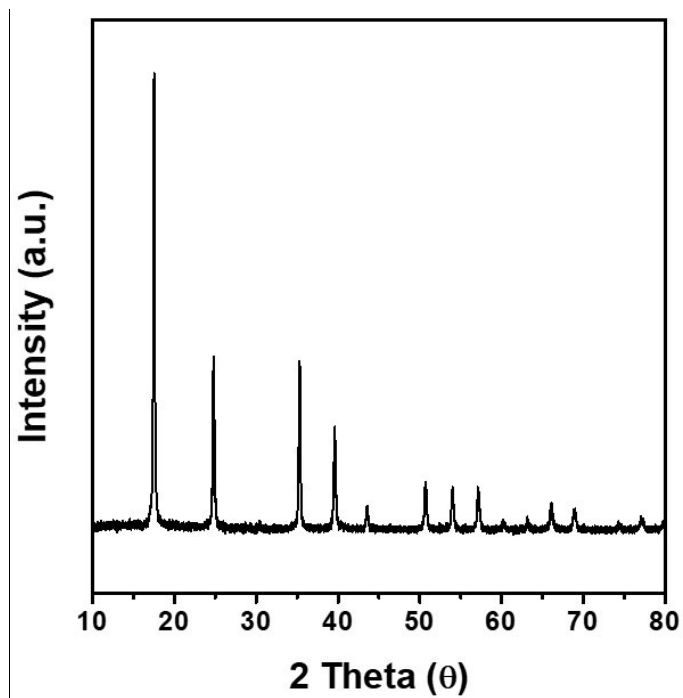
201

202

203

204

205



206  
207 **Fig. S2.** XRD pattern of synthesized PB.  
208

209

210

211

212

213

214

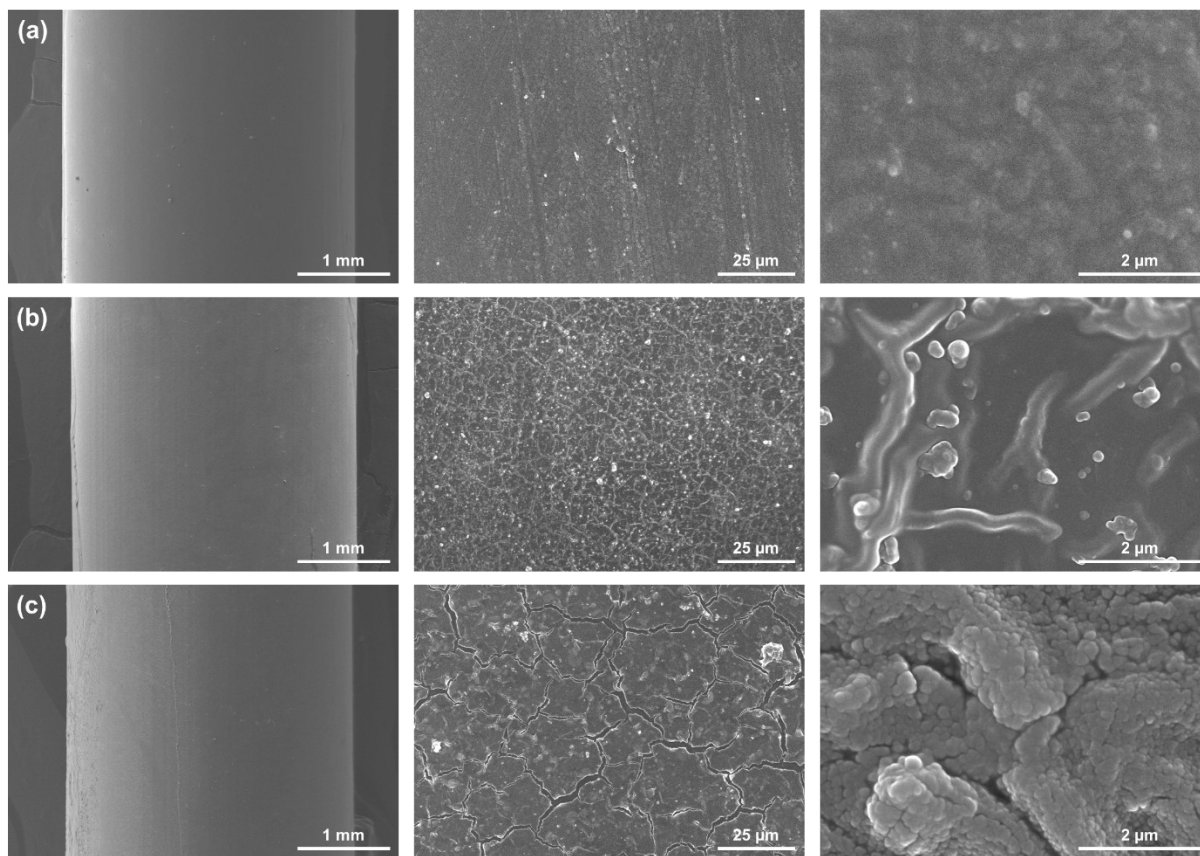
215

216

217

218

219



220  
 221 **Fig. S3.** Top-down view SEM images of (a) Tube, (b) Tube-D, and (c) Tube-D-PB at  $\times 30$ ,  $\times 1000$   
 222 and  $\times 20000$  magnifications.  
 223

224

225

226

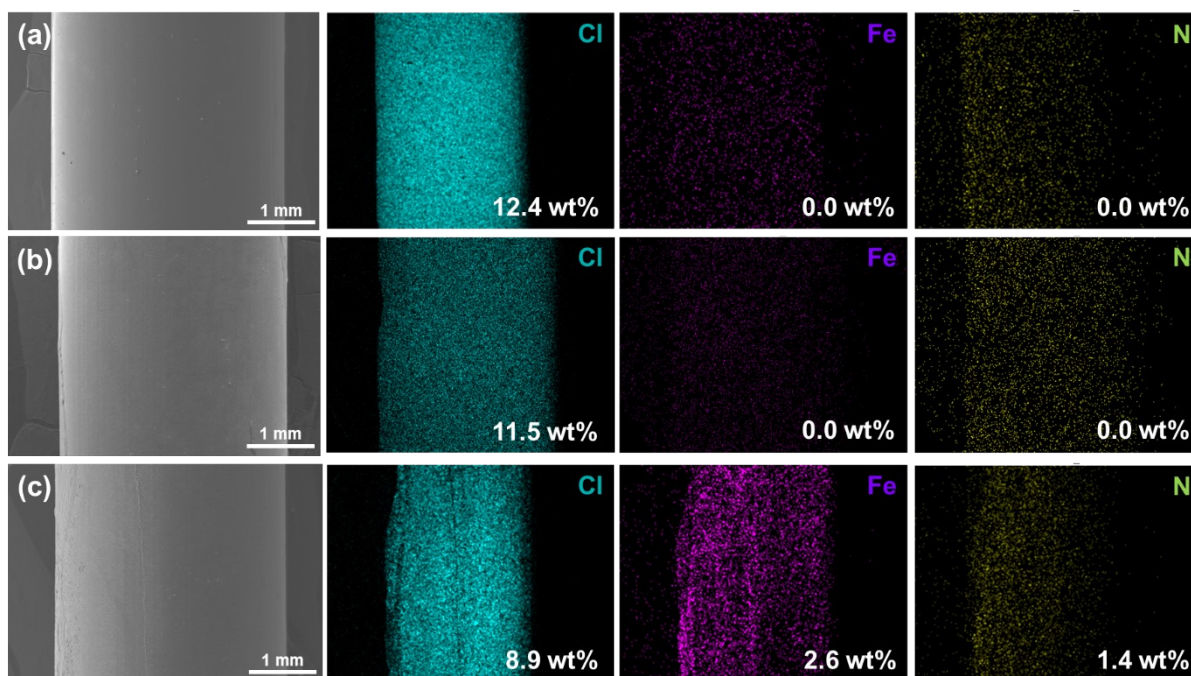
227

228

229

230

231



232  
 233 **Fig. S4.** Top-down view EDS mapping analysis of (a) Tube, (b) Tube-D, and (c) Tube-D-PB at  
 234  $\times 30$  magnification.  
 235

236

237

238

239

240

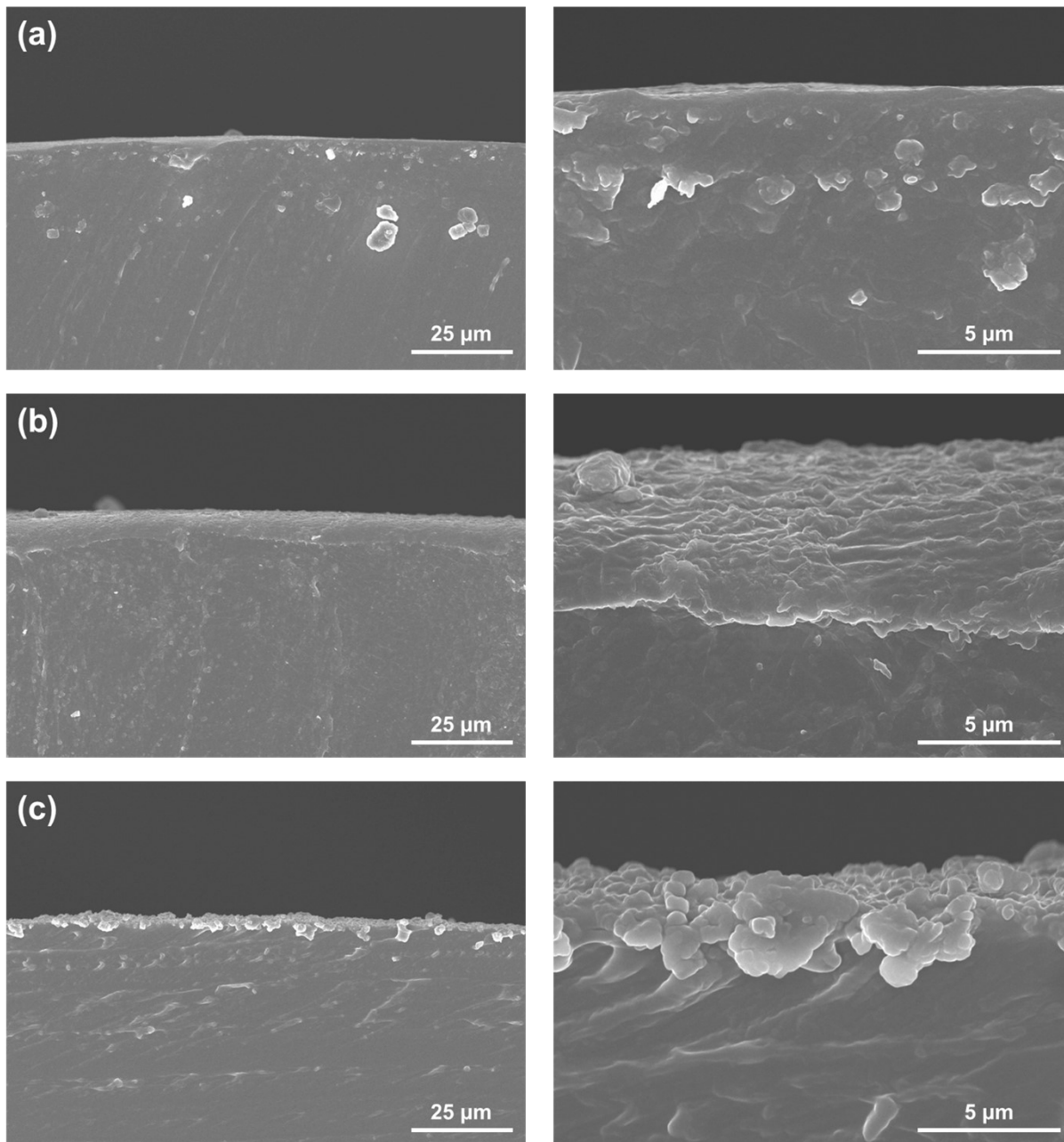
241

242

243

244

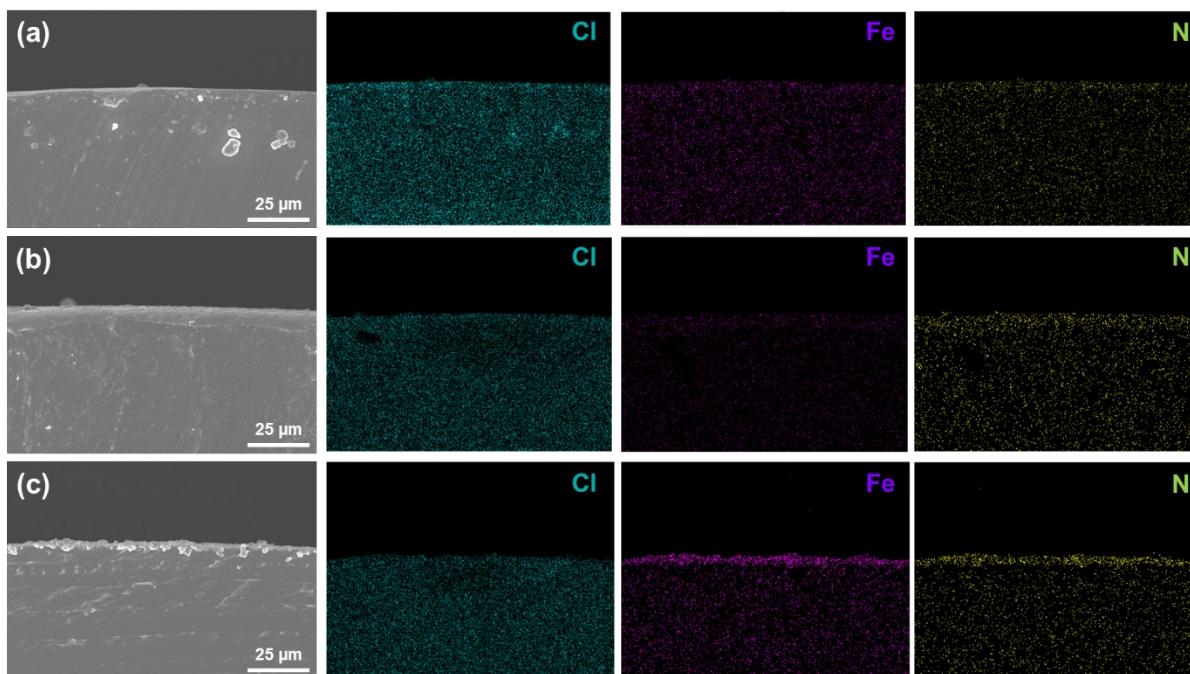
245



246  
247 **Fig. S5.** Cross-section view SEM images of (a) Tube, (b) Tube-D, and (c) Tube-D-PB at  $\times 1000$   
248 and  $\times 7000$  magnifications.  
249

250

251



252

253 **Fig. S6.** Cross-section view EDS mapping analysis of (a) Tube, (b) Tube-D, and (c) Tube-D-PB  
 254 at ×1000 magnification.

255

256

257

258

259

260

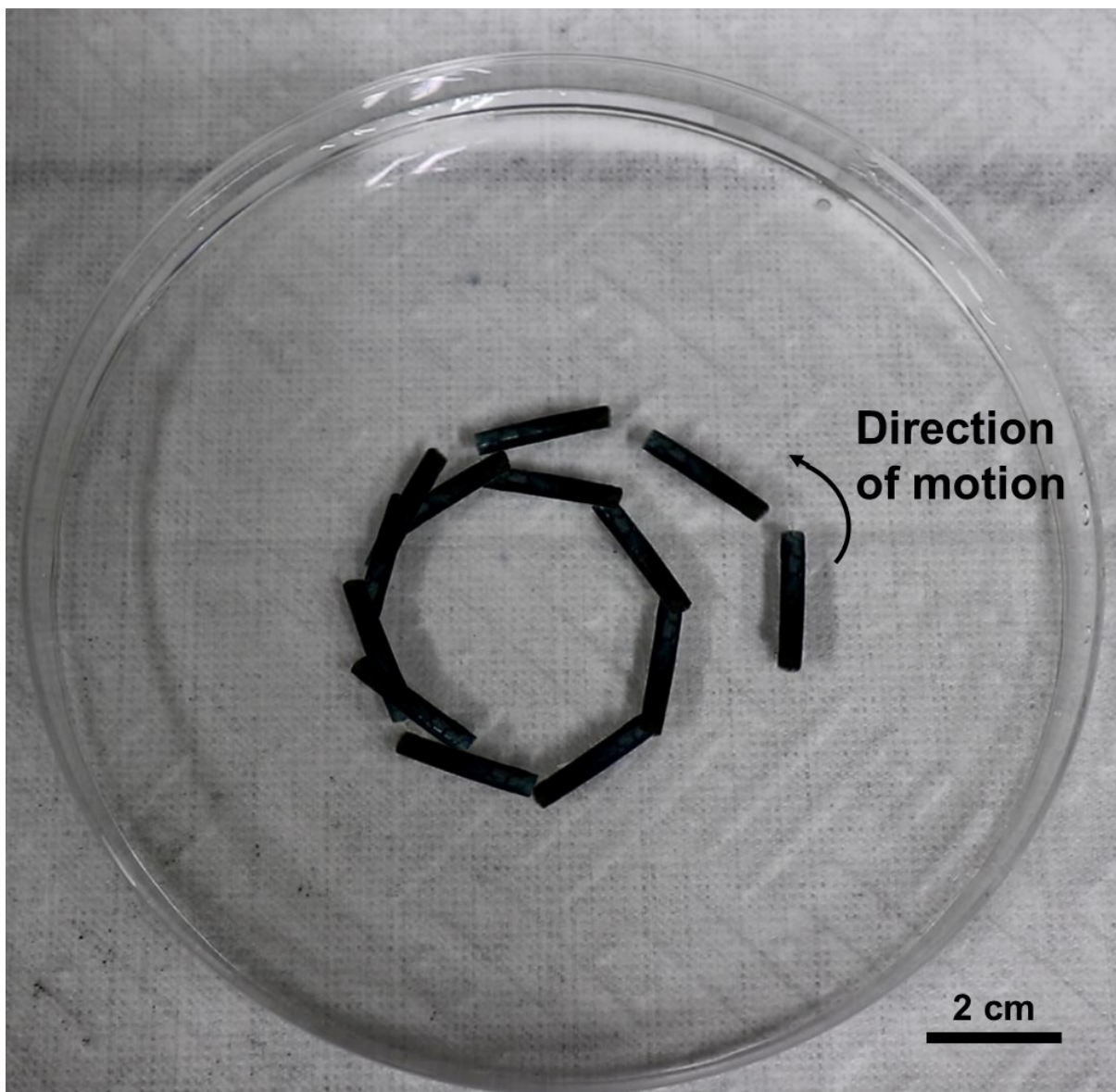
261

262

263

264

265



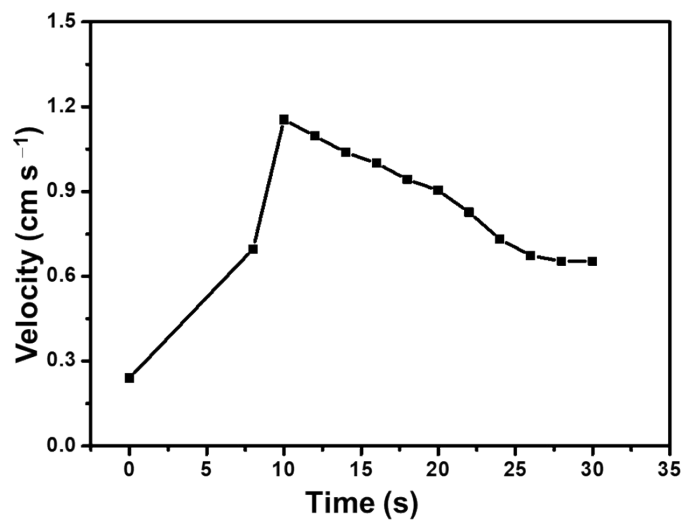
266  
267 **Fig. S7.** Photograph of the trace movement of Tube-D-PB in the aqueous system over a 15 second  
268 timeframe for illustration.  
269

270

271

272

273



274  
275 **Fig. S8.** Plot of the corresponding velocity of Tube-D-PB over a 30 seconds window.  
276

277

278

279

280

281

282

283

284

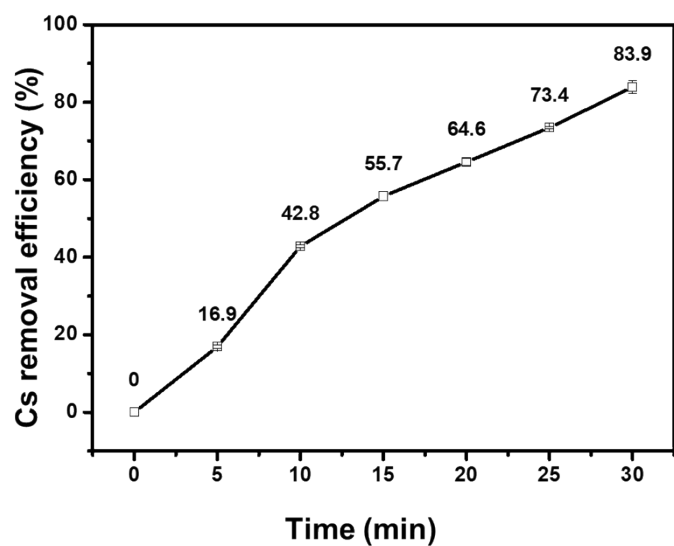
285

286

287

288

289



290  
291 **Fig. S9.** Cs removal test using a self-propelling Tube-D-PB coated with 1.0 M of  $\text{FeCl}_3 \cdot 6\text{H}_2\text{O}$  and  
292 functionalised with 0.5 M of  $\text{K}_4[\text{Fe}(\text{CN})_6] \cdot 3\text{H}_2\text{O}$  as a function of time.  
293

294

295

296

297

298

299

300

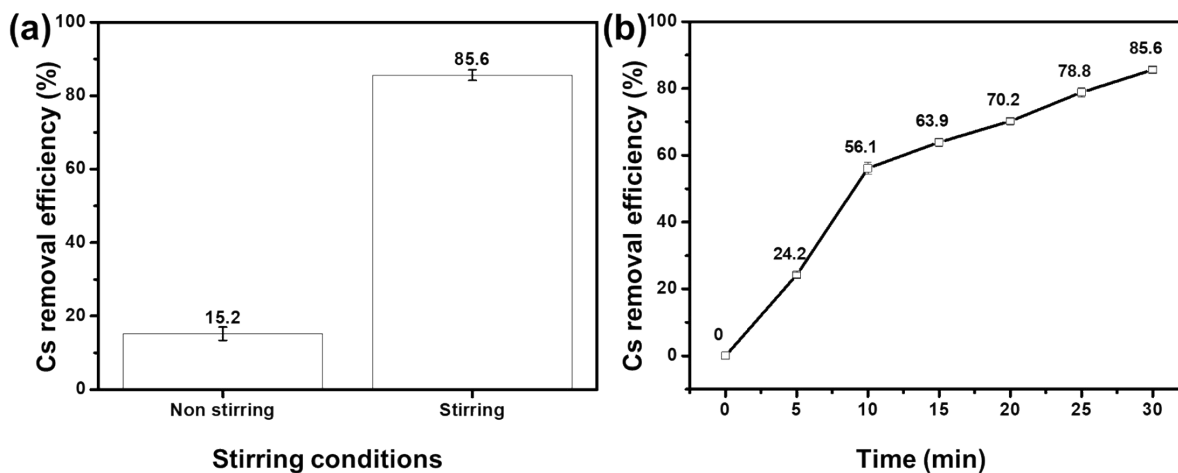
301

302

303

304

305



306  
 307 **Fig. S10.** Cs removal test using (a) dormant (non-self-propelling) Tube-D-PB under different  
 308 stirring conditions, (b) dormant (non-self-propelling) Tube-D-PB under stirring conditions as a  
 309 function of time.  
 310

311

312

313

314

315

316

317

318

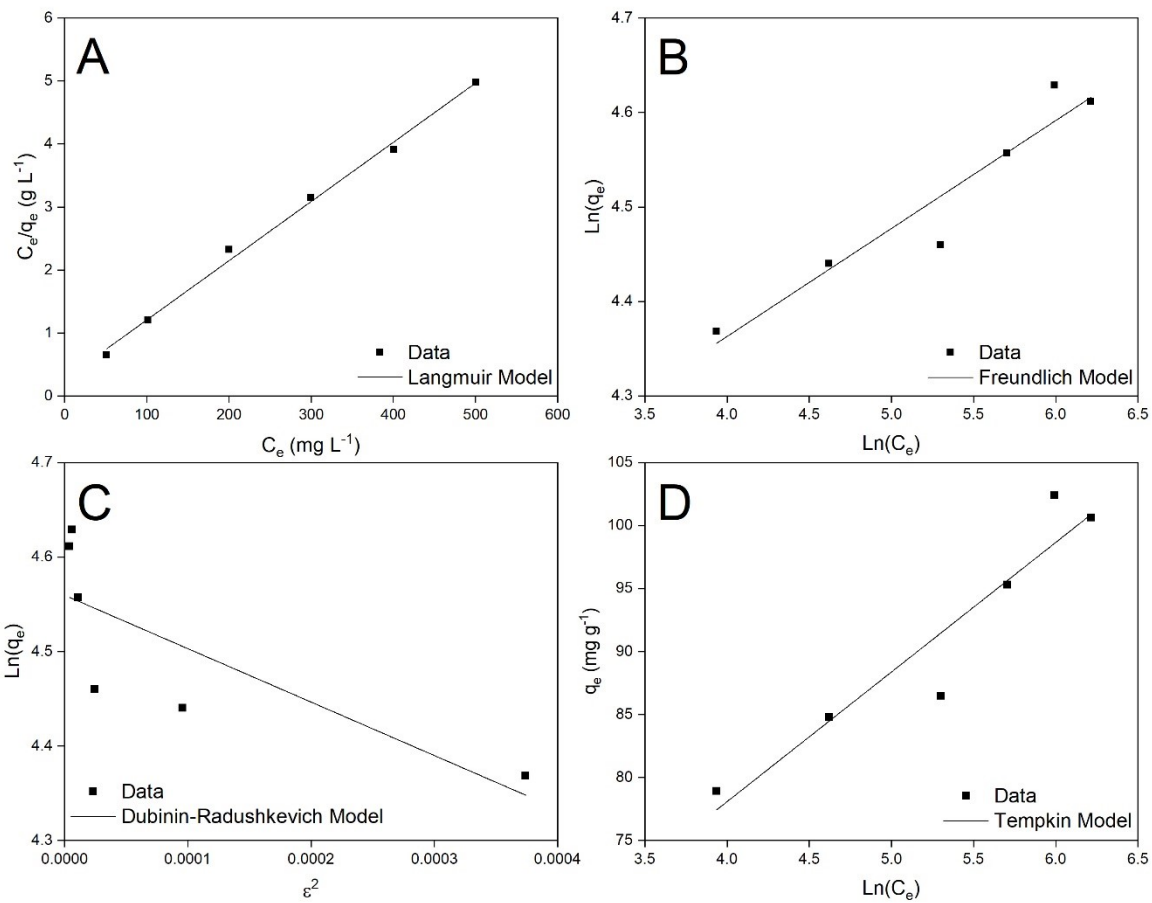
319

320

321

322

323



324  
 325 **Fig. S11.** Linear fits of selected adsorption isotherms (Langmuir,<sup>5</sup> Freundlich,<sup>6</sup> Dubinin-  
 326 Radushkevich,<sup>7</sup> and Tempkin<sup>8</sup>).  
 327

328

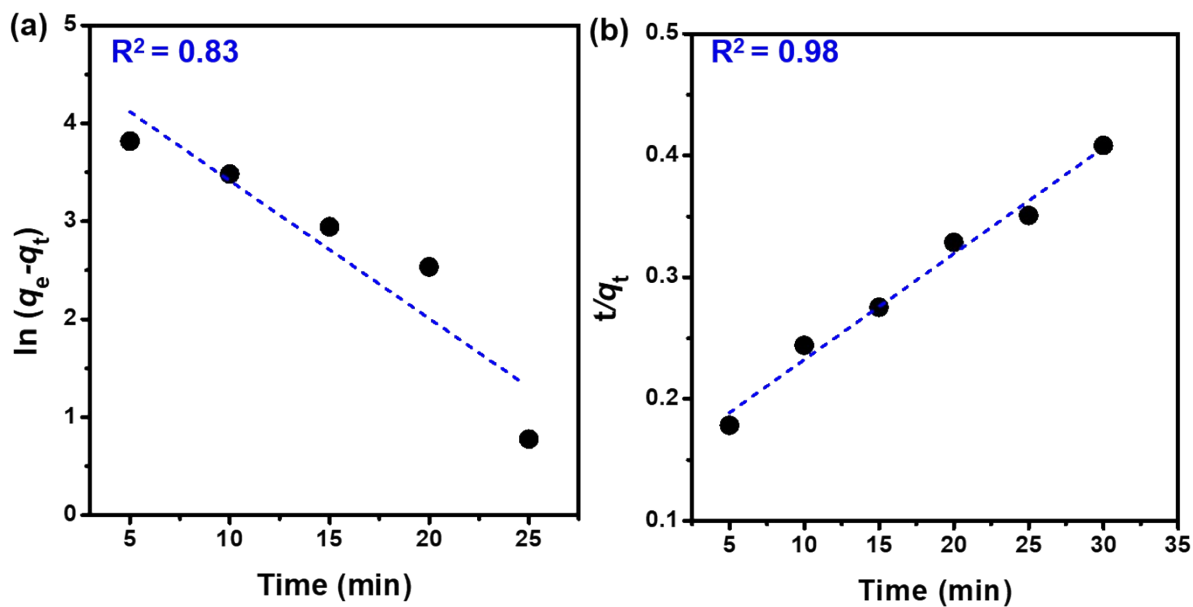
329

330

331

332

333



334  
 335 **Fig. S12.** (a) Pseudo-first-order vs (b) pseudo-second-order (50 ppm).  
 336

337

338

339

340

341 **Mov. S1.** Full movement of Tube-D-PB played back at four times the speed.

342

343

344

345

346

347

348

349

350 **IV. References**

- 351 1. Y.J. Gwon, J.J. Lee, K.W. Lee, M.D. Ogden, L.M. Harwood, T.S. Lee, Prussian Blue  
352 Decoration on Polyacrylonitrile Nanofibers Using Polydopamine for Effective Cs Ion  
353 Removal, *Ind. Eng. Chem. Res.*, 59 (2020) 4872–4880.
- 354 2. R. Sharma, S.T. Chang, O.D. Velev, Gel-based self-propelling particles get programmed  
355 to dance, *Langmuir*, 28 (2012) 10128–10135.
- 356 3. K.Y. Foo, B.H. Hameed, Insights into the modeling of adsorption isotherm systems,  
357 *Chem. Eng. J.*, 156(1) (2010) 2-10.
- 358 4. J.T.M. Amphlett, S.E. Pepper, A.L. Riley, L.M. Harwood, J. Cowell, K.R. Whittle, T.S.  
359 Lee, M.D. Ogden, Impact of copper(II) on activation product removal from reactor  
360 decommissioning effluents in South Korea, *J. Ind. Eng. Chem.*, 82 (2020) 261-268.
- 361 5. I. Langmuir, The constitution and fundamental properties of solids and liquids, *J. Am.*  
362 *Chem. Soc.*, 38(11) (1916) 2221–2295.
- 363 6. H.M.F. Freundlich, Over the adsorption in solution, *J. Phys. Chem.*, 57 (1906) 385–47.
- 364 7. M.M. Dubinin, L.V. Radushkevich, The equation of the characteristic curve of the  
365 activated charcoal, *Proc. Acad. Sci. USSR Phys. Chem. Sect.*, 55 (1947) 331–337.
- 366 8. M.I. Tempkin, V. Pyzhev, Kinetics of ammonia synthesis on promoted iron catalyst, *Acta*  
367 *Phys. Chim. USSR*, 12 (1940) 327–356.